Electronic Supplementary Material

Physiological thermal limits predict differential responses of bees to urban heat-island effects

April L. Hamblin, Elsa Youngsteadt, Margarita M. López-Uribe, and Steven D. Frank

I. Supplementary methods

Heat tolerance assay. CT_{max} is an ecologically relevant measure of heat tolerance that represents the point when an organism can no longer escape a stressful thermal environment [1]. Across ectotherms, it is also correlated with the harder-to-measure thermal optimum; in other words, species with high CT_{max} tend to have high thermal optima, such that CT_{max} should predict fitness changes even in response to sublethal temperatures [2].

To measure CT_{max}, we collected bees from university property and residential yards within 3.2 km of our laboratory, such that transit time from field to lab was no more than 10 min. Collecting sites were distinct from those used in the field population survey. We spent 15 – 35 min netting bees, which we transported individually in 50 ml plastic tubes in an insulated container. In the lab, we transferred bees to weighted 45 ml glass vials in a circulating water bath constructed from a 13.25 L tub equipped with a recirculation pump (Rio Plus 50 Aqua Pump, TAAM, Inc., Camarillo, CA, USA) and a heating element (120V, Camco, Greensboro, NC, USA) controlled by a JLD612 dual display PID temperature controller and PT100 temperature sensor probe (Lightobject, Sacramento, CA, USA). Vial openings, plugged with cotton, remained above water. Following an initial period of 20 min at 25 °C, the bath warmed at a rate of 0.5 $^{o}C\ min^{-1}$. The bath accommodated seven bees at a time, and we kept an additional one to seven bees per assay in a separate, unheated bath to ensure that experimental conditions other than heat were not lethal. To monitor temperatures experienced by bees, an iButton (DS1923, Maxim Integrated, San Jose, CA, USA) recorded temperature and humidity every minute throughout the assay within identical glass vials in the heated and control baths. We recorded the time at which each bee fell over and was unable to right itself within 30s. CT_{max} for each individual bee was the iButton temperature recorded during the minute that the individual lost

postural control. Because not all bees could be identified prior to the CT_{max} assay, species composition varied across trials; we present data for the 15 species that were common enough to yield at least 3 measurements per species.

***Field sampling*.** Site selection and sampling are described in detail elsewhere (Hamblin et al. in review). Briefly, we used Landsat-derived thermal map of Raleigh [3] to identify 15 residential yards and 3 urban natural areas that varied in warming intensity. Yards were 405 to 7487 m^2; natural areas were larger, but we limited sampling to 4047 m^2 per site. Residential neighborhoods were developed between the 1930s and 2003, such that local heat-island patterns were established at least a decade prior to sampling. All sites were more than 2 km apart to ensure independence of bee samples [4]. In 2015 we measured air temperature at each site using a pair of thermochron iButtons (DS1921, Maxim Integrated). Despite shielding iButtons as described by Hubbart [5], daytime readings were compromised by solar radiation. We therefore used only early evening temperatures (7-9pm) to compute a mean summer evening temperature at each site. Although this temperature does not represent conditions experienced by foraging bees, it captures the urban heat island effect without interference from solar radiation, accurately arraying sites on an axis from cooler to warmer [6].

We sampled bees from May to August, visiting each site 6 times in 2014 and 5 times in 2015. At each site on each date we deployed 12 pan traps and 1 blue vane trap (SpringStar, Seattle, WA), and conducted 20 min of netting. Pan traps were 3.25 oz soufflé cups (Solo Cup Co., Urbana, IL), left white or painted fluorescent yellow or blue (Guerra Paint & Pigment, New York, NY). On each sampling date, traps were out for 5 to 7 hours between 8:00 and 17:30 and we netted between 10:00 and 17:00. The full bee sample, described elsewhere, included 113 species, most of which were rare; here we focus on the 15 common species for which we also

measured CT_{max}. For these 15 species, the total number of individuals collected was 1732 (n = 11 – 549 per species). In all downstream analyses, the abundance of a given species at a given site refers to the total number of individuals of that species collected over the two years of sampling.

Hierarchical model. To estimate the rate of change in abundance of each species relative to temperature, we constructed a hierarchical model analogous to a Poisson regression with log link function: $\log(\mu_{ij}) = a_i + r_i * t_j$ where μ_{ij} is the predicted count (a Poisson mean) for the ith species at the jth site; a_i is the intercept for species i, r_i is the Poisson regression coefficient for species i, and t_j is the temperature at site j. The coefficient r_i represents proportional change in abundance of a species per °C increase in temperature, and we refer to it as "response to warming" throughout this study. (Specifically, for each 1°C increase in temperature, μ is multiplied by e^{r_i}.) We further specified r_i as arising from a normal distribution with mean β and variance σ^2, so that responses of all species were estimated jointly relative to the overall, species-wide response, β. This approach allowed information from the entire dataset to inform the estimates for each species, stabilizing estimates for rarer taxa [7,8]. We fit the model in WinBUGS 1.4, assuming uninformative prior distributions for a, β, and σ^2. We used 3 Markov chain simulations, each independently initialized and computed for 21000 draws. After inspecting diagnostic plots for convergence and autocorrelation, we discarded the first 1000 draws from each chain and thinned to every tenth draw for a final sample of 6000 draws, which we used to compute estimates, standard errors, and 95% credible intervals for each species' response to warming (r_i).

Phylogenetic inference. We downloaded the 20 gene dataset generated by Hedtke et al. [9], and selected one outgroup (*Dasypoda hirtipes*) and the lineages of interest for our study. Eleven of the 20 genes contained less than 10% of sequence data for our ingroup, thus we

removed those genes from our dataset. We included the following nine genes in our study: arginine kinase (AK), calcium/calmodulin-dependent protein kinase II (CAD), elongation factor 1-α copy 1 and 2 (EF1a1, EF1a2), sodium potassium adenosine triphosphate (NAD), phosphoenolpyruvate carboxykinase (PEPCK), long wavelength rhodopsin (Opsin), RNA polymerase II (PolII), and wingless (Wg). We added sequence data from the mitochondrial gene cytochrome oxidase I (COI) to improve species level resolution within the genera *Bombus* and *Megachile*. COI sequences for all species were retrieved from the National Center for Biotechnology Information (NCBI) or the BOLD System (table S1). We used sequences from the phylogenetically closest species when sequences from the focal species were not available. We aligned COI nucleotide sequences using the MUSCLE option in SeaView v.4.5.3 [10] and concatenated to nine-gene dataset [9]. Phylogenetic reconstruction was based on a total of 10,252 nucleotides in our final alignment. Alignments were visually inspected and improved in Mesquite 3.0.3. Maximum likelihood trees were searched under the GTRGAMMA model of sequence evolution in RAxML using 1000 bootstrap replicates after partition optimization using the python script PartitionFinder v1.1.1 [11]. Trees were visually inspected and annotated in FigTree v.1.4.2 (http://tree.bio.ed.ac.uk/).

Table S1. COI sequences and genbank accession numbers. These sequences were concatenated to 9 genes from Hedtke et al. [9].

Species in this study	Species in Hedtke et al.	Species for COI	COI Genbank Accession No.
Agapostemon virescens	*Agapostemon kohliellus*	*Agapostemon virescens*	JQ266376
Bombus bimaculatus	*Bombus bimaculatus*	*Bombus bimaculatus*	KM585629
Bombus griseocollis	*Bombus griseocollis*	*Bombus griseocollis*	SMTPL8163*
Bombus impatiens	*Bombus wilmattae*	*Bombus impatiens*	JF799030
Ceratina calcarata	*Ceratina calcarata*	*Ceratina calcarata*	KJ166268
Ceratina strenua	*Ceratina cyanea*	*Ceratina strenua*	KJ163420
Halictus ligatus	*Halictus ligatus*	*Halictus ligatus*	AF102840
Lasioglossum bruneri	*Lasioglossum cressonii*	*Lasioglossum bruneri*	JF903499
Lasioglossum imitatum	*Lasioglossum imitatum*	*Lasioglossum imitatum*	AF103967
Megachile campanulae	*Megachile angelarum*	*Megachile cetuncularis*	FJ582307
Megachile exilis	*Megachile angelarum*	*Megachile versicolor*	KJ836926
Megachile mendica	*Megachile patellimana*	*Megachile mendica*	KF839683
Megachile rotundata	*Megachile texana*	*Megachile rotundata*	GU706002
Ptilothrix bombiformis	*Ptilothrix sp. JS 2010*	*Ptilothrix bombiformis*	AF300562
Xylocopa virginica	*Xylocopa virginica*	*Xylocopa virginica*	EU271670

* Retrieved from BOLD system

II. Supplementary results

Hierarchical model of species responses to warming. The assemblage-wide mean response to warming was significantly negative with $\beta = -0.66$ (95% CI -0.96 to -0.40). Within this overall trend, species varied in their rates of decline; four species' responses were indistinguishable from zero (as indicated by 95% credible intervals, fig. S1).

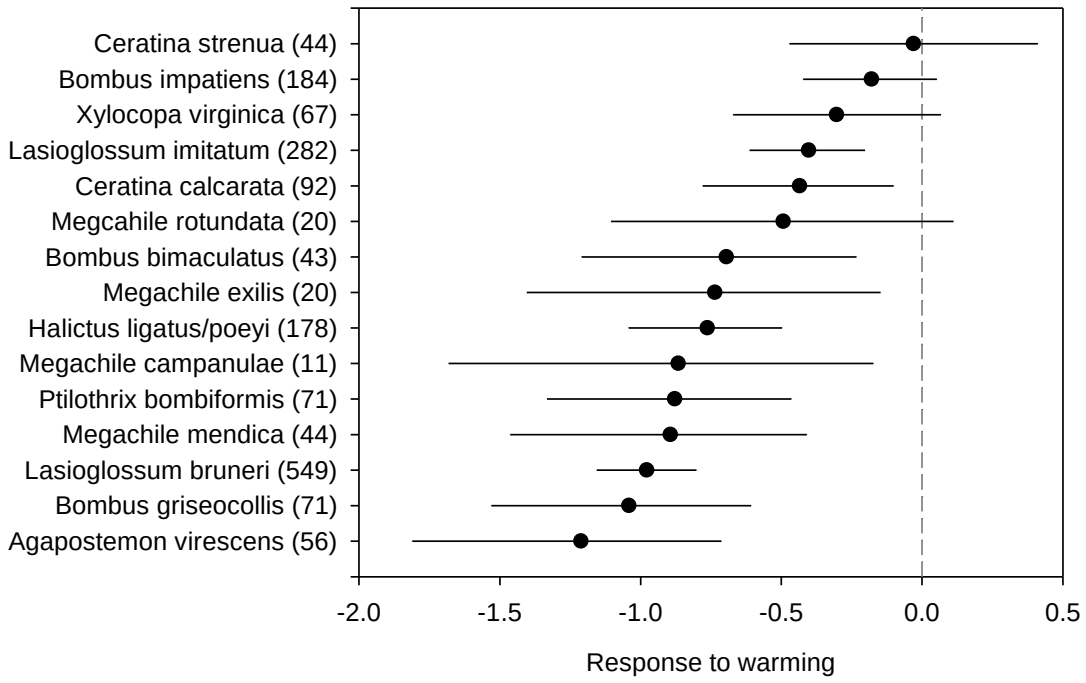

Figure S1. Results of hierarchical model estimating Poisson regression coefficients for each bee species ("response to warming" as rate of population change per °C). Error bars are 95% credible intervals; numbers in parentheses are total number of individuals collected.

Phylogeny reconstruction. We reconstructed the phylogenetic relationships of 21 bee species from four families using information from one mitochondrial and nine nuclear genes (fig. S2). The maximum likelihood phylogenetic reconstruction recovered all bee families with high bootstrap support, and the tree topology is congruent with Hedtke et al.

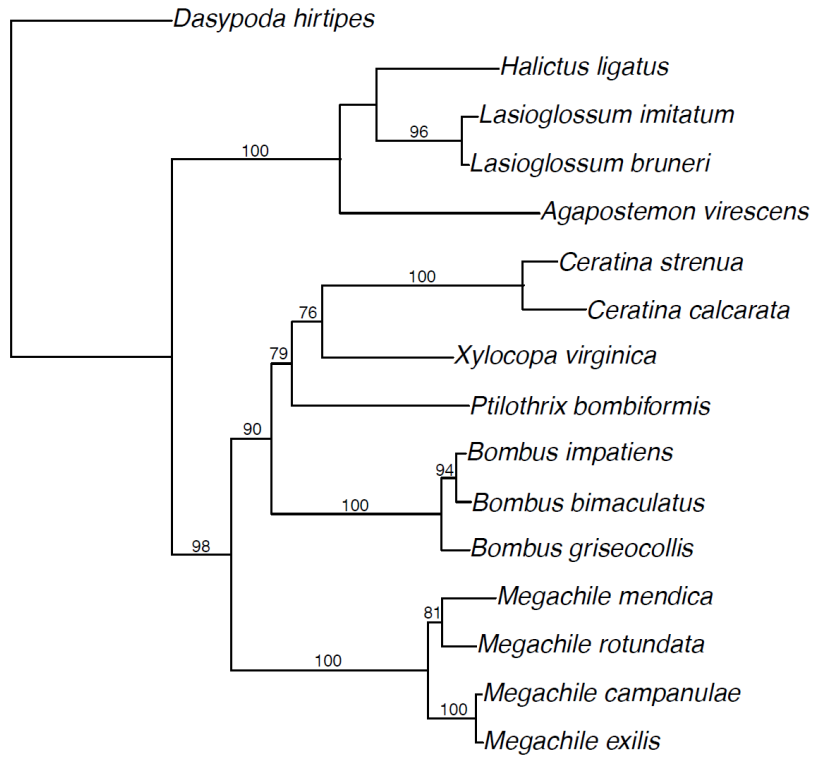

Figure S2. Phylogenetic reconstruction of 15 focal bee species; numbers on branches are bootstrap values after 10000 replicates.

Trait evolution. The relationship between phylogeny, CT_{max}, nesting behavior, and sociality is shown in fig. S3. We did not detect strong phylogenetic signal in CT_{max}; that is, models of trait evolution that incorporated the phylogeny were not a better fit to the data than was a phylogenetically independent white-noise model (ΔAICc <2, table S2). Body size, nesting habitat, and social behavior were all phylogenetically correlated; Brownian motion and Early Burst were the best-supported models of trait evolution (tables S2-S3).

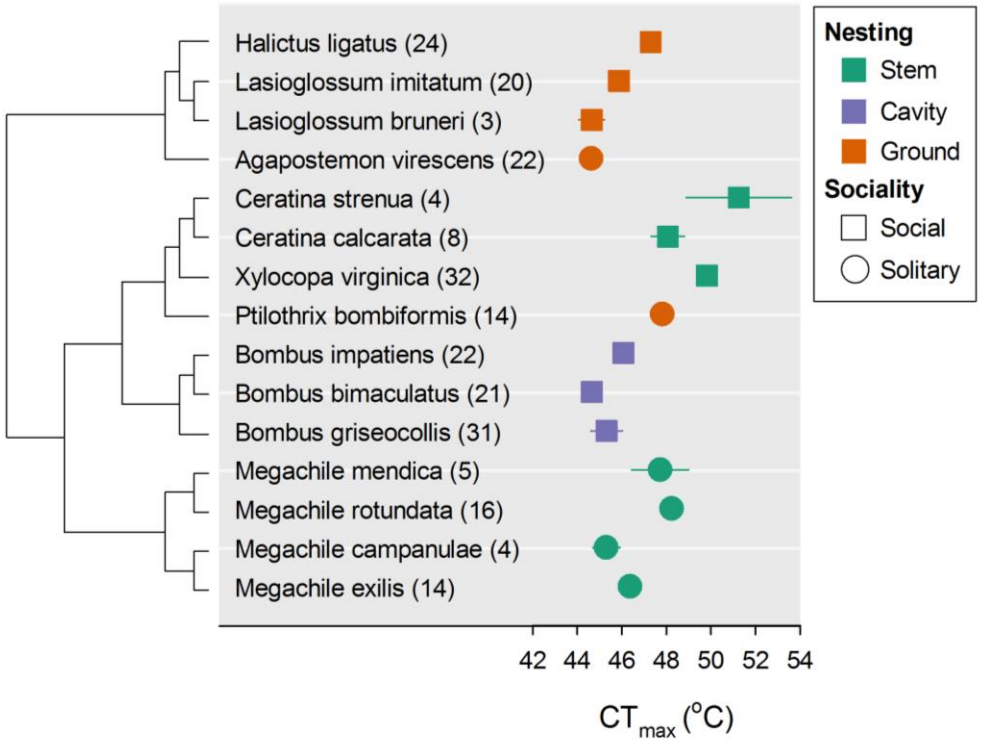

146

147 Figure S3. Bee traits considered in this study, as they relate to the phylogeny (numbers in

148 parentheses are sample sizes for CT_{max} assay).

149

150 Table S2. Models describing trait evolution of CT_{max} and body size across the bee phylogeny.

151 Best-fitting models (ΔAICc <2) for each trait are bolded.

	CT_{max}			Body size		
Model	AICc	ΔAICc	Parameters	AICc	ΔAICc	Parameters
Brownian motion	**67.37**	**0.99**	**σ^2 = 23.59**	**50.29**	**0.00**	**σ^2 = 7.56**
Ornstein-Uhlenbeck	**66.38**	**0.00**	**σ^2 = 46.48, α = 5.76**	53.36	3.07	σ^2 = 8.93, α = 0.82
White noise	**66.95**	**0.57**	**σ^2 = 3.64, μ = 46.87**	60.59	10.30	σ^2 = 2.38, μ = 2.70,
Pagel's λ	**66.66**	**0.28**	**σ^2 = 9.69, λ = 0.78**	53.47	3.18	σ^2 = 7.56, λ = 1.00
Early burst	70.55	4.17	σ^2 = 23.59, a = 1.00×10^{-6}	53.28	2.99	σ^2 = 15.03, a = -2.01

152

153

154

Table S3. Models describing trait evolution of discrete traits, nesting habitat and sociality, across the bee phylogeny. Best-fitting models (ΔAICc <2) for each trait are bolded.

Model	Nesting				Sociality			
	AICc	ΔAICc	Parameters	Rate[1]	AICc	ΔAICc	Parameters	Rate[2]
Equal-rate models								
Brownian motion	19.98	2.42	NA	0.68	**15.21**	**0.00**	**NA**	**1.48**
White noise	36.31	18.80	NA	NA	22.50	7.29	NA	NA
Pagel's λ	22.67	5.11	λ = 1.00	0.68	17.90	2.69	λ = 1.00	1.48
Early burst	**17.56**	**0.00**	**a = -28.06**	**978.17**	**15.84**	**0.63**	**a = -20.15**	**978.17**

Phylogenetic generalized least-squares models. Regardless of the pattern of evolution of individual traits, the residuals of models relating those traits to one another (as in our two focal hypotheses) can also show phylogenetic signal. We addressed this possibility by comparing several models that differed only in their phylogenetic covariance structure. In the main text, we present the results of the best-fitting models; in Table S4 we provide fit details for the alternative models.

Table S4. Comparison of generalized least-squares models testing two hypotheses with different phylogenetic correlation structures.

Model	Phylogenetic correlation structure	d.f.	Log likelihood	AICc	ΔAIC_c	Model weight
CT_{max} ~ Body size + Nest + Sociality	Pagel's λ	7	-0.3	30.6	0.0	1.0
	None	6	-25.1	72.6	42.0	0.0
	Ornstein-Uhlenbeck	7	-24.5	79.0	48.4	0.0
	Brownian motion	6	-30.1	82.7	52.1	0.0
Response to warming ~ CT_{max}	None	3	-0.3	8.7	0.0	0.8
	Ornstein-Uhlenbeck	4	0.05	11.9	3.2	0.2
	Brownian motion	3	-6.6	21.3	12.62	0.0
	Pagel's λ	did not converge*				

*Although the Pagel's λ model did not converge using the gls function in nlme package in R, and therefore is not included for direct comparison with the other gls models, we examined a comparable model with Pagel correlation structure using the pgls function in the caper package, which produced a maximum-likelihood estimate of $\lambda = 0$ (95% CI 0 to 0.594). We also manually fit different values of λ in the gls function, and likelihood was maximized at $\lambda = 0$. These checks support the conclusion that there is not strong phylogenetic signal in the relation between response to warming and CT_{max}.

Weighted regression. To examine the possibility that error in the estimation of species responses to warming influenced our analysis of the relationship between CT_{max} and response to warming, we further examined the non-phylogenetic model using weighted regression. We weighted each response to warming by the inverse of its standard error (as estimated in the hierarchical model), thereby reducing the influence of the least certain estimates. We fit the weighted regression using the lm function in the stats package of R. Results (table S5) were comparable to those of the non-weighted regression shown in the main text.

Table S5. Results of weighted regression describing each species' response to warming as a function of its CT_{max} (where each response is weighted by the inverse of its standard error).

Term	**Coefficient**	**s.e.**	***t***	***p***
Intercept	-5.52	1.86	-3.0	**0.011**
CT_{max}	0.10	0.040	2.6	**0.021**

III. Community Analysis

The results of the hierarchical model demonstrate that some bee species declined faster than others in response to warming. These differential rates of change imply that species' relative abundances, and thus community composition, also shifted with warming. Here, we explicitly test for an effect of temperature on bee community composition across sites by performing a distance-based redundancy analysis (db-RDA) using the vegan package in R [12]. This constrained ordination analysis assumes a linear relation between predictors (here, temperature) and the multivariate response (bee abundances), and tests significance with a permutation test (without assuming multivariate normality) [13,14]. In this analysis, we log(x+1) transformed bee counts to meet the assumption of linearity, and used db-RDA with Bray-Curtis distances because the Euclidean distances of standard RDA are misleading when the data include many zeros [13].

The db-RDA detected significant effects of site temperature on community composition across sites, with 14% of the inertia in the dataset represented on the db-RDA axis that aligns with temperature ($p = 0.015$, fig. S4). Species' loadings on the temperature axis could be analyzed as an alternate quantification of "response to warming" that makes the connection between CT_{max} and community ordination more explicit. For ease of interpretation, however, we focused our analyses on the Poisson regression coefficients, for which error is more readily estimated and which represent rate of change in biologically meaningful units.

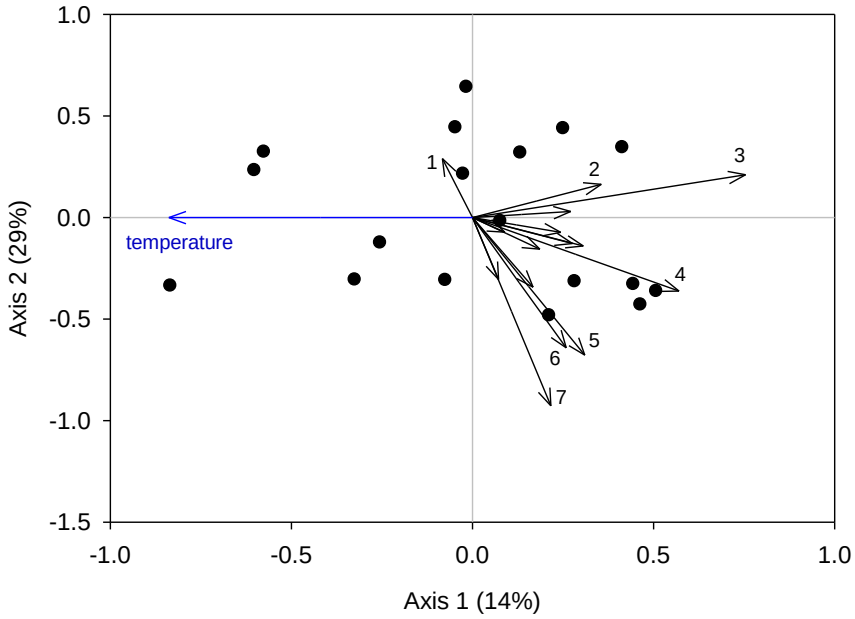

Figure S4. db-RDA ordination indicates that bee community composition varied across sites as a function of temperature. Black points represent the positions of the 18 study sites in ordination space, as they relate to temperature (blue arrow) and bee species abundances (black arrows). Arrows indicate the direction of increase of each variable; the plot was generated using scaling = 3 to optimize display of sites and species. For clarity, only selected species are labeled. They are 1, *Ceratina strenua*; 2, *Ceratina calcarata*; 3, *Lasioglossum bruneri*; 4, *Bombus griseocollis*; 5, *Agapostemon virescens*; 6, *Megachile mendica*; 7, *Halictus ligatus/poeyi*.

References Cited in the Supplementary Material

1. Lighton, J.R. & Turner, R.J. 2004 Thermolimit respirometry: an objective assessment of critical thermal maxima in two sympatric desert harvester ants, *Pogonomyrmex rugosus* and *P. californicus*. *J. Exp. Biol.* **207**, 1903-1913.

2. Huey, R.B. & Kingsolver, J.G. 1993 Evolution of resistance to high temperature in ectotherms. *Am. Nat.*, S21-S46.

3. Meineke, E.K., Dunn, R.R., Sexton, J.O. & Frank, S.D. 2013 Urban warming drives insect pest abundance on street trees. *PLoS ONE* **8**, e59687.

4. Greenleaf, S.S., Williams, N.M., Winfree, R. & Kremen, C. 2007 Bee foraging ranges and their relationship to body size. *Oecologia* **153**, 589-596.

5. Hubbart, J.A. 2011 An inexpensive alternative solar radiation shield for ambient air temperature and relative humidity micro-sensors. *Journal of Natural and Environmental Sciences* **2**, 9-14.

6. Meineke, E., Youngsteadt, E., Dunn, R.R. & Frank, S.D. 2016 Urban warming reduces aboveground carbon storage. *Proc. R. Soc. B* **283**, 20161574.

7. Gotelli, N.J., Dorazio, R.M., Ellison, A.M. & Grossman, G.D. 2010 Detecting temporal trends in species assemblages with bootstrapping procedures and hierarchical models. *Philos. Trans. R. Soc. B* **365**, 3621-3631.

8. Kruschke, J.K. 2015 *Doing Bayesian Data Analysis: A Tutorial with R, JAGS, and STAN*. London, Academic Press.

9. Hedtke, S.M., Patiny, S. & Danforth, B.N. 2013 The bee tree of life: a supermatrix approach to apoid phylogeny and biogeography. *BMC Evol. Biol.* **13**, 138.

10. Gouy, M., Guindon, S. & Gascuel, O. 2010 SeaView version 4: A multiplatform graphical user interface for sequence alignment and phylogenetic tree building. *Mol. Biol. Evol.* **27**, 221–224.

11. Lanfear, R., Calcott, B., Ho, S.Y. & Guindon, S. 2012 PartitionFinder: combined selection of partitioning schemes and substitution models for phylogenetic analyses. *Mol. Biol. Evol.* **29**, 1695-1701.

12. Oksanen, J., Blanchet, F.G., Friendly, M., Kindt, R., Legendre, P., McGlinn, D., Minchin, P.R., O'Hara, R.B., Simpson, G.L., Solymos, P., et al. 2016 Vegan: community ecology package. R package version 2.4-1. Available at: CRAN.R-project.org/package=vegan.

13. Legendre, P. & Legendre, L. 2012 *Numerical Ecology*. Amsterdam, Elsevier.

14. Gotelli, N.J. & Ellison, A.M. 2004 *A Primer of Ecological Statistics*. Sunderland, Massachusetts, USA, Sinauer.